Brite-EuRam project 6001

Contract No. BRE2 CT92 0340

Development of high quality linear low density polyethylene and optimised processing for film blowing

Publishable Synthesis Report

Period :
from 1-XI-1992 to 30-IV-1996

Distribution list

Dow Benelux N.V. :	Dr. R. Koopmans, Dr. D. Liebmann
Reifenhäuser GmbH :	B. Schroeter & B. Reckmann
Polyflow s.a. :	Dr. B. Debbaut, Dr. J.M. Marchal, Dr. A. Goublomme & O. Homerin
Hyplast N.V. :	P. Verschaeren
École des Mines :	Prof. J.-F. Agassant, Dr. B. Vergnes &C. Venet
ETH-Zürich :	Prof. J. Meissner

Development of high quality linear low density polyethylene and optimised processing for film blowing

B. Debbaut[1], A. Goublomme[1], O. Homerin[1], R. Koopmans[2], D. Liebmann[2], J. Meissner[3], B. Schroeter[4], B. Reckmann[4], T. Daponte[5], P. Verschaeren[5], J.-F. Agassant[6], B. Vergnes[6] and C. Venet[6]

[1] Polyflow s.a., Place de L'Université 16, B-1348 Louvain-la-Neuve, Belgium
[2] Dow Benelux N.V., Polyolefins R & D, P.O. Box 48, NL-4530 AA Terneuzen, The Netherlands
[3] Eidgenössiche Techn. Hochschule Zürich, Institut fur Polymere, CH-8092 Zurich, Switzerland
[4] Reifenhäuser GmbH, Maschinenfabrik, Spicher Straße 46-48, D-53839 Troisdorf, Germany
[5] Hyplast N.V., St-Lenaartseweg 16, Postbus 14, B-2320 Hoogstraten, Belgium
[6] École des Mines de Paris, CEMEF, Sophia-Antipolis, F-06560 Valbonne, France

Abstract

The majority of LLDPE resins is processed via blown film extrusion techniques for various applications in the industrial and consumer packaging business. These LLDPE resins all have, independent of the molecular structure differences, the same intrinsic Imitation in blown film extrusion processing. These limitations are : low output, high sensitivity to surface defects (stripes, sharkskin), high machine power requirement, need for large die gaps, lower bubble stability, and low melt strength. As a consequence, the more versatile –manufacturing and property wise– LLDPE resins are not used to their full potential.

The industrial objective is therefore threefold :
- develop a new LLDPE resin overcoming the above limitations,
- develop a new flexible blown film extrusion line tailored to the new generation of LLDPE resins,
- develop an efficient 3D Finite Element Simulation code to assist in the resin and blown film extrusion line development.

Key words: Film blowing – Extrusion – LLDPE resins – Surface defects – Numerical simulation

---

1. Introduction

The intrinsic melt flow limitations of LLDPE in present blown film extrusion are reflected mainly in bubble instability and surface defects. The present remedies such as larger die gaps and special additives –processing aids (PA)- and LDPE/LLDPE blends, limit the economic and technical potential of LLDPE.

Recent developments in resin manufacturing have indicated two viable solutions to overcome these difficulties. (i) : Use of multiple reactor production technology to broaden the molecular weight distribution of LLDPE and thus improving processability and final film properties [1-5]. (ii) : Single reactor homogeneous catalyst technology offers compared to the classic Ziegler-Natta heterogeneous catalyst more tailoring of the molecular structure with respect to molecular weight- and comomomer-distribution, resulting in LLDPE resins not showing flow instability at current shear stresses of 90 000 to 150000 Pa [6-9].

The key technology in both approaches is the control over the high molecular weight tail of the polydisperse polymer, i.e. the molecular weight (>1,000 000 g/mol) and the amount of these molecules. The rationale is the specific fractional contribution of the relaxation time related to this molecular weight tail with respect to the shear rate or output of the machine as described by Vinogradov et al. for polybutadienes and polyisoprenes [10]. Furthermore, the viscosity - shear rate curve must show a stronger shear-thinning behaviour matching that of LDPE and HDPE, as shown in Fig. 1, in order to achieve optimum process ability [11]. A broadening of the molecular weight distribution which will be reflected in similar shear-thinning behaviour as for LDPE and HDPE can be achieved with a multiple reactor technology.

From the extrusion blown film process, the technical limitations in LLDPE processing have several origins : the too high shear stresses in the die lips which result in surface defects (sharkskin), the gauge distribution which depends on the flow behaviour in the spiral mandrel, and eventually the too low capacity of conventional cooling system which leads to bubble instability. Developing a modular system with adaptable modules –single screw extruder, spiral mandrel die, air-cooling system– allows to select the correct modules for optimum extrusion blown film line performance. These improvements will allow to achieve a lower melt processing temperature and an acceptable die pressure drop, combined with the absence of surface defects and an intensified film cooling. The degree of innovation in the extrusion blown film machine for achieving these objectives will reside in the design of : (i) a high output low torque single screw system, (ii) the modular modification of the spiral-mandrel die, and (iii) the cooling system. In the present context, advanced numerical methods need to be used.

The numerical simulation of the complete extrusion and film blowing process requires major capabilities. First of all, simulating the flow of complex polymers such as LLDPE in processes involving free surfaces requires the use of a multi-mode differential viscoelastic fluid model, with or without coupling to the energy equation [12]. The current computer and solver technologies allow such a complex simulation for a single-mode fluid model [13]. However, computational time and memory requirements make it impossible to simulate such flows with a multi-mode viscoelastic fluid model. Further, in view of the complex flow geometries, it is essential to analyse the process in three dimensions. 3-D free surfaces are available [14], but such simulations require a large CPU time, mainly because the present solver is based on a Gaussian

2

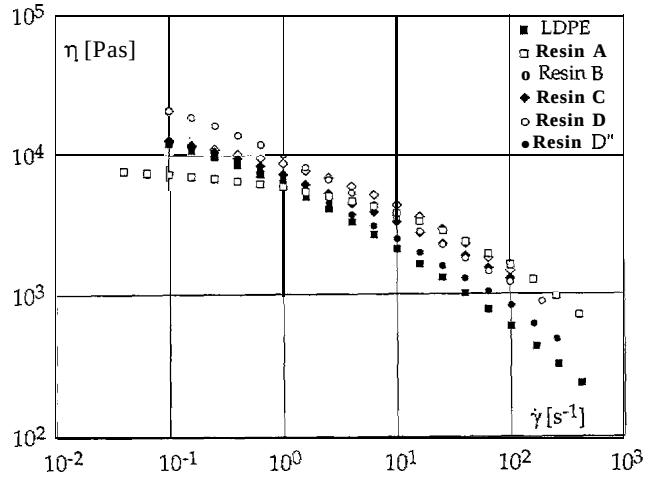

Fig. 1. Shear viscosity of the LDPE, the reference resin A and the successive resins B to D".

elimination. 3-D viscoelastic simulations including free surfaces represent a new challenge for numerical simulation, in view of the present efficiency limitations of the solver. Several techniques will be explored for overcoming these limitations. The solver performances will be improved by the implementation of a Schur complement technique combined with a parallel algorithm based on a computational domain decomposition.

As stated above, a major limitation in film blowing process originates from surface defects. Actually, Many defects are observed in extrusion : sharkskin and spurt defects, gross melt fracture. The appearance of defects has been delayed by modifying the die geometry or by introducing additives into the polymer, while their true origin remains an open debate: slip conditions, viscous behaviour, compressibility, wave propagation [15-17]. In this project, major research efforts will focus on surface defects called sharkskin or haze, as encountered at low flow rates for LLDPE. In particular, attempts will be carried out in three main directions : (i) to study the occurrence of defects on real industrial installations, (ii) to correlate the occurrence of defects between complex die flow and simple capillary flow, (iii) to calculate complex flows of polymers as close as possible to reality and to estimate critical parameters for the occurrence of surface defects. In the present context, the use of simplified numerical models will allow to test the various hypotheses.

2. Resin manufacturing and optimisation

To set the base line in processing and film property performance, a reference LLDPE Dowlex™* NG5056E was selected, and referred to as resin A. This resin was fully characterised from a molecular structure and theological viewpoint. In particular, intensive measurement campaigns have led to a complete knowledge of the resin rheology. The shear viscosity was obtained in both capillary and oscillatory viscometry, and is displayed in Fig. 1. For high shear rate, as encountered in the extrusion line, the shear viscosity is too high, and leads thus to temperature increase due to viscous heating. The extensional

* Trademark of the Dow Chemical Company

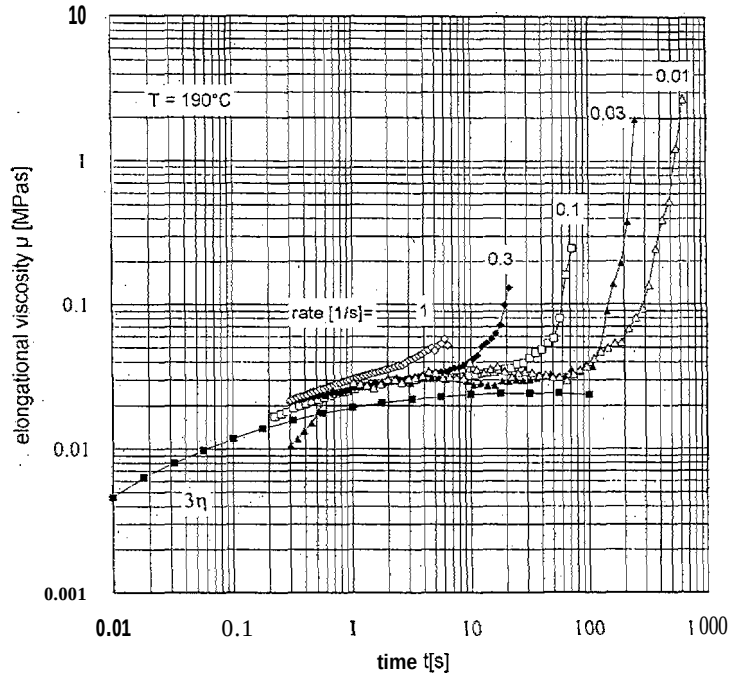

Fig. 2. Transient extensional viscosity for the standard reference LLDPE.

viscosity is an important property, as it affects the bubble stability in film blowing process. Extensional data of the reference resin have been obtained by means of the advanced Meissner extensional rheometer [18], and are displayed in Fig. 2. Further, this resin was evaluated on existing Reifenhäuser GmbH extrusion blown film line in order to quantify the processing performances in terms of maximum throughput, melt temperature and pressure. Optical and mechanical properties of the blown film produced at Reifenhäuser GmbH and Hyplast N.V. were also determined

From these results, guidelines for resin developments were set-up. To explore the possible molecular structures which could be made in relation to their final performance, a designed experiment following the Box-Behnken [19,20] method was carried out. Successive intermediate resins were designed and produced on a small scale (20-25 kg). They were next evaluated in order to identify the most viable option amongst many possible ones, keeping in mind the final feasibility and manufacturing cost. New resins were produced with gradually improved processing and end-use properties. It was ultimately possible to design a new LLDPE exhibiting the same processing behaviour as LDPE but with enhanced blown film performance.

All new resins were produced by means of metallocene catalyst technology. Currently the metallocene catalyst technology is more expensive than the classical Ziegler-Natta catalyst. However, it allows enhanced design control over molecular weight, molecular weight distribution and inclusion of branching. A higher molecular weight affects the crystallisation, and thus the optical properties : crystallisation is more rapid resulting in increased haze.

It is important here to point out that a balance needs to be found between processability and optical properties. Indeed, long chain branching affects the

rheology while short chain branching affects the optical properties. Based on this, a design for the final resin has been selected. Fig. 1 compares the shear rheology of the reference resin (A), an LDPE and the several resins developed for designing the final resin. A clear distinction can be made with the reference LLDPE, and the final resins D“ and D. The lower viscosity at higher shear rates reflects the better process-ability of the newly developed resins. In terms of extensional properties, significant improvement have also been accomplished. Fig. 3 displays the transient extensional viscosity obtained at various extension rates for an LDPE and both resins A and D as well. *One* finds that resin D exhibits an enhanced extensional behaviour, and this will affect the blown film performances. This final resin D has been produced on a large “ scale. Industrial trials have been carried out on both the existing extrusion line and on the new one. Performance results are presented below in section 6.

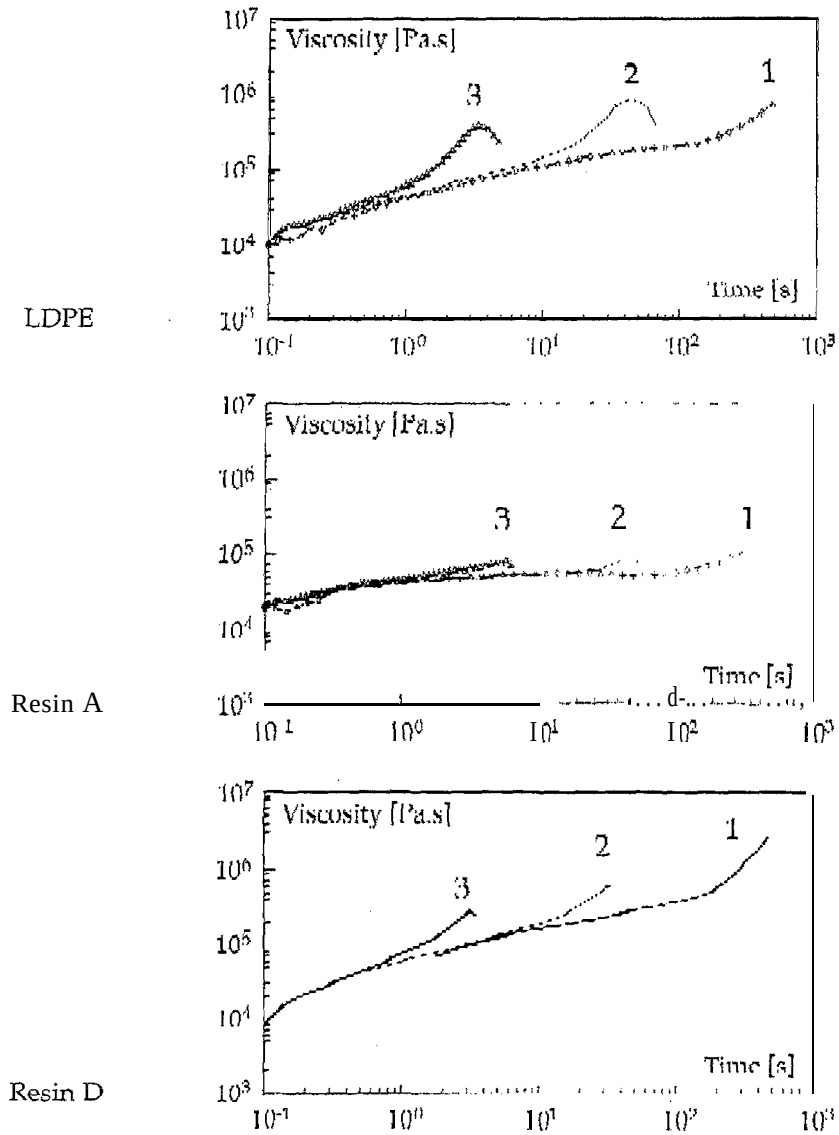

Fig. 3. Transient extensional viscosity obtained at various extension rates : (1) $\dot{\varepsilon}$ = 0.01 S-l, (2) $\dot{\varepsilon}$ = 0.1 S-l, (3)&=1 S-l. Time ranges between 10^{-1} and 10^{3} s.

3. Extrusion line design and optimisation

3.1. Screw optimisation

In view of the several possible parameters for describing a screw geometry, preliminary simulations were carried out with the use of a global 1-D model available in the *Cemextrud* package [21]. This approach allows a quick and efficient analysis for a lot of virtual screw designs, and provides guidelines for the optimisation Procedure. First of all, the performances of the existing extrusion lines have been simulated. Further geometric and process parameters were varied for optimisation purposes. The resin rheology was also changed in order to account for the new developments in this context. Eventually it allowed to identify the best possible combination of geometric parameters. A typical sketch of a screw design is shown in Fig. 4.

These 1-D simulations provide global information on important variables such as pressure and temperature along the screw. Hence it is important to perform a detailed analysis with a full 3-D simulation. The simulation package *Polyflow* [13] has been enhanced with additional models and numerical tools, as described below in section 4. The numerical calculations have led to a detailed knowledge of the flow around the screw. In particular, it has allowed to show that temperature non-uniformities remain between the acceptable limit of 5 °C. At this time, several designs are suggested for the feeding and mixing parts of the screw, and only experimental trials allow to select the best design.

The first criterion for evaluating a screw is its specific throughput, i.e. the ratio of the throughput to the screw speed. The specific throughput should be independent of the screw speed, in other words the characteristic curve of the screw should be horizontal. In the present situation, it is found that the specific throughput is constant, except at a screw speed of 20 rpm where higher values can be observed. For both resins A and an intermediate C, it has been

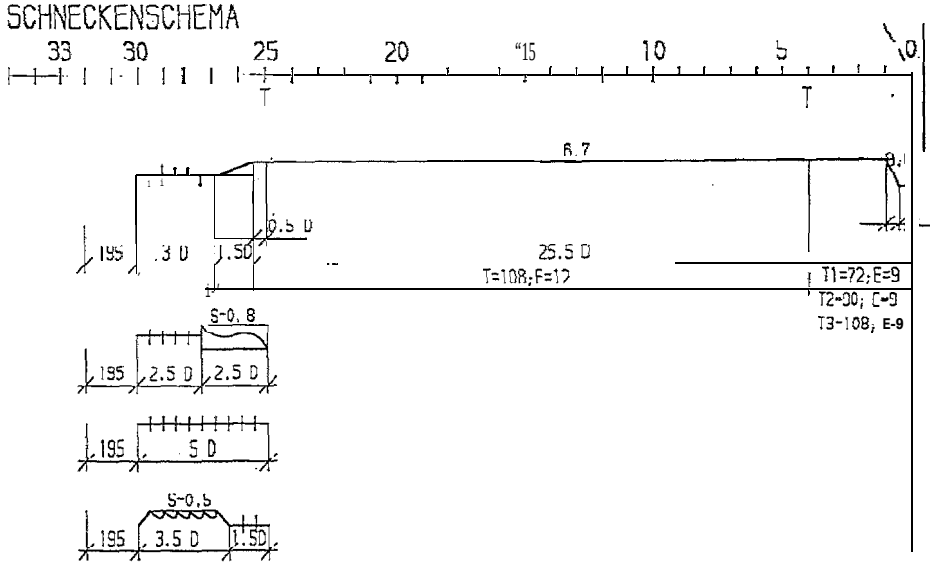

Fig. 4. Sketch of the screw

experimentally observed that the specific throughput is improved with a pitch of 1.0. The second criterion is the melt temperature, which should be as low as possible. It is measured after the screen changer located in the middle of the adapter channel. Here too, a pitch of 1.0 leads to the lowest melt temperature which is even lower with resin C than with the reference resin.

3.2. *Optimisation of the spiral mandrel die and die lips ; internal cooling system.*

The objectives of the optimisation procedure for the spiral mandrel die are the homogeneity of the temperature field, the control of both axial and circumferential flow rates, the residence time distribution and the reduction of the pressure drop.

A similar strategy was followed as for the optimisation of the extrusion screw. Indeed, a lot of parameters are needed for describing the spiral mandrel die geometry, and it is necessary to use an efficient technique for identifying the more relevant ones and their respective effects in order to select the best design for the spiral mandrel die. In this context, the *Figaine* software was used [21]. The residence time distribution is an important output of the simulation. It is based on the tracking of a large number of material points, typically 1000 markers are selected, which allow to obtain statistical information on the residence time distribution. Further information are related to the circumferential flow rate distribution.

Amongst the several geometrical parameters of the spiral mandrel die, the most important ones were identified and considered for pursuing the optimisation procedure. An optimised design was then selected. Next, further 3-D calculations were carried out with the use of the *Polyflow* software, in order to refine the results and again obtaining detailed information on the flow. In this context, a specific model has been developed for the combined simulation of flows in channels and gaps. Compared to its initial counterpart, the new spiral mandrel die essentially differs by a lower channel depth (i) accompanied by a higher slope at the inlet to the channel (ii), and by a larger gap at the channel exit (iii).

A further detailed analysis of the results has shown that the circumferential flow rate distribution is basically sinusoidal, with a period of 45°, resulting from the eight entry channels. A final simulation was performed for a modified new die with a "counter-sinusoidal" profile of the gap at the die exit in order to balance the sinusoidal flow rate profile. The solution results have shown a significant improvement, with relative flow rate variations lower than 2%. Unfortunately, the magnitude of the corresponding suggested modifications are of the same order than the manufacturing tolerance errors, and hence could not be applied for technological reasons.

Beyond the die lips, the polymeric material enters into contact with air, and the film bubble is formed. Cooling is an important ingredient in order to obtain the desired film, and hence must be properly adjusted. There are generally three possible ways to increase the cooling capacity for high melt

throughput. (i) By increasing the air velocity, but this leads quickly to bubble instability. (ii) The air flow rate can also be increases; a new internal bubble cooling stabiliser has been assembled which overcomes the troubles originating form velocity distribution. (iii) Finally, cooled air can be used. At high throughput, it has appeared that the best solution for cooling improvement consists of using cold air, the temperature of which lies between 0 and 5 'C. This allows to keep a stable bubble while maintaining the frost line at an acceptable location on the bubble.

4. Numerical simulation of three-dimensional viscoelastic flows

4.1. Numerical algorithm

As stated above, a lot of large numerical simulations had to be performed for obtaining a detailed description of the melt flow in the extruder and in the spiral mandrel die. Initially, a frontal based direct solver (with Gaussian elimination) was used. Its major advantages are its robustness and its easiness, in the sense that it always produces the solution of a linear system of unknowns without the need of parameter tuning. **A** major drawback is the significant computational time and memory requirements for solving large 3-D flow cases.

In this context, the target is to develop a new solver which overcomes these requirements. This must be achieved without modifying the mathematical formulations of the equations to solve, while keeping the advantages of the Newton iteration scheme. Also the new solver must be able to solve saddle-point problems, as typically encountered for incompressible fluid flows. More generally, it must be able to handle incompressible 3-D viscoelastic flows with moving boundaries, and involving more than 100000 variables. Parallel implementation must also be considered. The Schur complement method with a possible coupling to an iterative solver will be investigated.

The Schur complement method is based on a domain decomposition which leads to a decoupling of the system on a sub-domain basis rather-than on a component basis. There is an obvious reason for this. All unknowns in an element (stress, velocity and pressure) exhibit a strong local coupling which makes a decoupling on a component basis less attractive. Moreover, unknowns in a part of the domain show a loose coupling with unknowns in another part of the domain. Hence relationships between unknowns must be solved locally with a robust solver, and the direct solver remains the most robust one, whereas the system resulting from the assembling of the Schur complements (interfaces of the domains) can be solved either with a direct or an iterative solver.

The Schur complement algorithm coupled with the direct solver can be applied for solving the majority of flow situations with the *Polyflow* package. Unfortunately, for large flow problems, memory usage is not really reduced. Moreover, for a lot of sub-domains (e.g. 32) handled with a lot of processors, the parallel efficiency is rather poor.

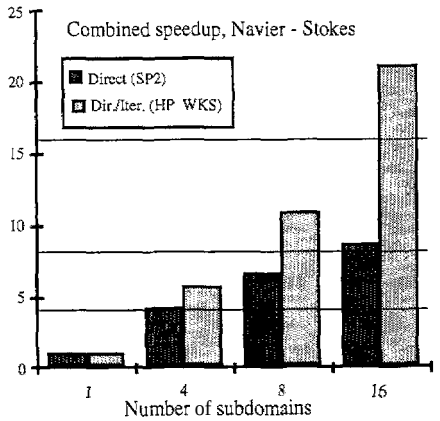

Fig. 5. Speed-up for 3-D Navier-Stokes problem involving 50000 variables.

The parallel implementation of the Schur complement iterative method reduces both the memory requirements (size and use) and the computation time for large problems (> 100000 unknowns). Moreover, theoretical results showed that the condition number of the system is improved when unknowns are previously eliminated on a sub-domain basis. Here, the Schur complement technique acts as an efficient preconditioned for the iterative solver.

An iterative solver cannot be directly applied to the original system to be solved, in view of the resulting bad memory usage and swapping. Additionally, a corresponding preconditioning step is time consuming. The iterative technique presently used is based on the GMRES algorithm [22-27]. As such, the GMRES solver cannot be applied to saddle point problems, as typically encountered for incompressible fluid flows. Indeed, the condition number of the system is poor and affects the convergence rate. In order to circumvent these difficulties, a modified version of the GMRES has been developed. The basic idea consists of modifying the linearised system

$$A\,x = b$$

into

$$A'\,x = b'$$

where A' is now positive-definite, and is obtained by internal products and is characterised by a better condition number. It is important to note that the same unknowns are solved. The positive-definiteness of A' improves the convergence rate. When the Schur complement technique is used, the evaluation of A' is performed together with the matrix-vector product, and the corresponding time is negligible as compared to a matrix-vector product.

It was observed that the combination of the Schur complement technique with the modified GMRES iterative solver is the best candidate for a parallel implementation. All processes build one or more Schur complements in parallel, while matrix-vector products can be performed blockwise. If the matrix A results from several Schur complements A_i, all matrix-vector products can be performed in parallel at the level of the Schur complement :

$$A\,v = \sum_i A_i\,v$$

In view of this property, the system of equation solved by means of the iterative solver does not need to be assembled, and several small and non-sparse matrices are kept into memory without using any pointer structure. The memory requirement for each processor remains in acceptable limits.

The implemented parallel strategy is based on a dynamic distribution of tasks (Schur complements, matrix-vector products, etc.). This strategy is very adaptive: it limits the transfer of large table between processes and performs an automatic load-balancing. Hence a complex domain decomposition algorithm is not needed. Instead, the program Chaco developed by the Sandia National Laboratories [28] was selected for the domain decomposition.

The performances of this new solver are impressive : significant speed-up are observed, as indicated in Fig. 5. The speed-up is evaluated as the ratio of the elapsed time on several processes to the elapsed time on one process; the elapsed time includes disk access and transfer between processes. Using the Schur complement technique, speed-ups of about 8 and 21 have been achieved with the direct solver and the iterative solver, respectively.

4.2. *A mathematical* formulation *for the spiral mandrel die*

An appropriate mathematical model for the simulation of complex flows in a single screw extruder or in a spiral mandrel die should involve leakage flows. These leakage flows are typically encountered between the screw thread and the barrel or in the gap of a spiral mandrel die. Here an acceptable discretisation would require a high number of elements, in relation to the specific geometry of the gap and of the main flow area. Hence numerical analyses of such flows were so far limited by the tremendous number of 3-D finite elements necessary.

A new approach has been developed. It consists of coupling both 3-D Navier-Stokes and 2-D Hele Shaw [29] equations on their respective

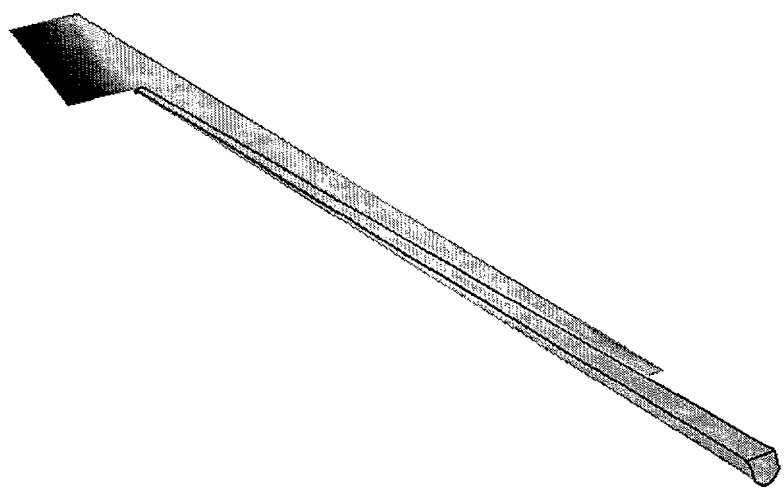

Fig. 6. Pressure distribution of the coupled model (3-D / 2-D) of the spiral mandrel die

computation domains (the channel and the gap). These domains are now only connected along a line. This coupling technique guarantees the continuity of the pressure between both computation domains as well as the conservation of the mass flow rate.

Fig. 6. displays one eighth of the unwrapped geometry for a spiral mandrel die. Pressure distribution for both 3-D Navier-Stokes and 2-D Hele Shaw calculation domains can be observed. In particular, it is found that the pressure is continuous across the connecting line. A similar mathematical model has been applied for the optimisation of the spiral mandrel die, where leakage flows are an important part for the melt distribution.

5. Surface defects analysis and quantification

As stated above in the text, surface defect (shark skin) is a severe limitation in blown film extrusion. For the successive resins, several measurements have been performed in order to quantify the occurrence of surface defects. Capillary rheometry experiments have provided an important number of samples : for all resins, 3 temperatures, 2 L/D ratios, and 24 output rates were tested. Extruded samples were rapidly cooled down in water at the die exit, indeed slow cooling in air would have enabled relaxation of the extrudate surface. Optical microscopy measurements were performed on the reference resin A, on an intermediate resin C and on two monodisperse resins (linear) CGC957 and (short chain branched) CGC870 with well characterised molecular structure, in order to be able to quantify the observed behaviour.

Microscopic observations have allowed to define a classifications of surface defects, namely: smooth / mat / sharkskin / spurt / smooth / rough / volume distortion / chaotic. Amongst these observations, sharkskin has retained a lot of efforts. It appears with alveolus (at low throughput) or stripes (at high throughput). Amplitude and period may characterise the phenomenon.

Further, it has been necessary to quantify the sharkskin development. This was done on the basis of optical microscopy, profilometry, and cross-

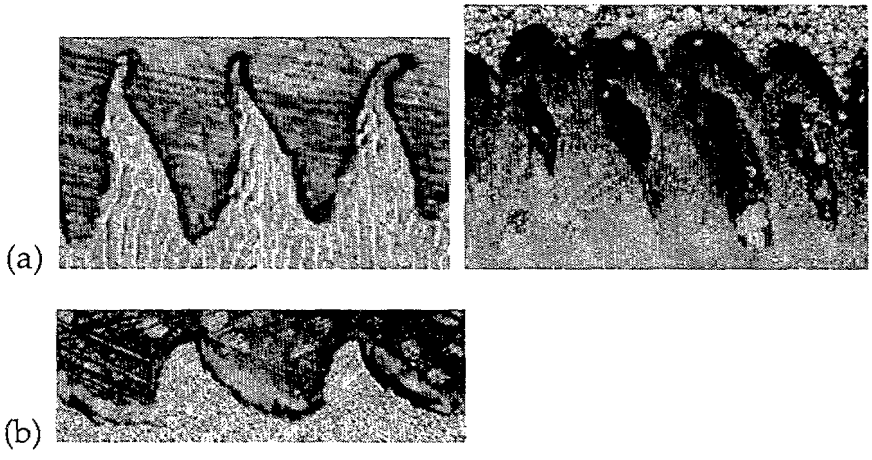

Fig. 7. Typical cross-sections of extrudate surfaces : L/D=0 (a), L/D=16 (b)

section analysis of samples. Mechanical roughness measurements allow also to precisely identify the occurrence of mate surface, whilst optical measurements are necessary for detecting the occurrence of sharkskin. .4s displayed in Fig. 7, the aspect ratio of the capillary strongly affect the development of sharkskin.

A precise quantification of surface defects aHows the direct comparison of the resins in terms of surface extrudate quality. This has been done for all four resins considered above in the section, with different temperatures and capillary geometry. It has been observed that shear-rate leads to' an increase of both amplitude and period of sharkskin, while a temperature increase improves the surface quality. These measurements also showed that short chain branching influences the occurrence of sharkskin. Finally resin C, precursor to the final resin as discussed in section 2, shows the best behaviour in terms of extrudate quality.

A numerical simulation of the flow through a capillary die has also been simulated. In this context, the 2-D axisymmetric model involves also the development of the free jet at the die exit. A Phan Thien-Tanner differential viscoelastic fluid model with a relaxation spectrum has been selected [30]. The objective of the numerical simulation is to understand the development of sharkskin defect in connection with an estimation of the values for strain and stretch rates along the free surface. At the capillary exit, the velocity profile is rearranged, from a Poiseuille-like profile in the die to a bulk-like profile in the extrudate. The elongation at the free surface near the die exit and the stresses created at this point are supposed to be linked to the sharkskin defect. Cracks, due to the breaking of the surface, may be initiated under critical stresses or critical strain rates. Their development can then lead to sharkskin defect. The tangential velocity, the elongation rate and the tangential stresses are computed along the free surface. With the assumption that the surface defect

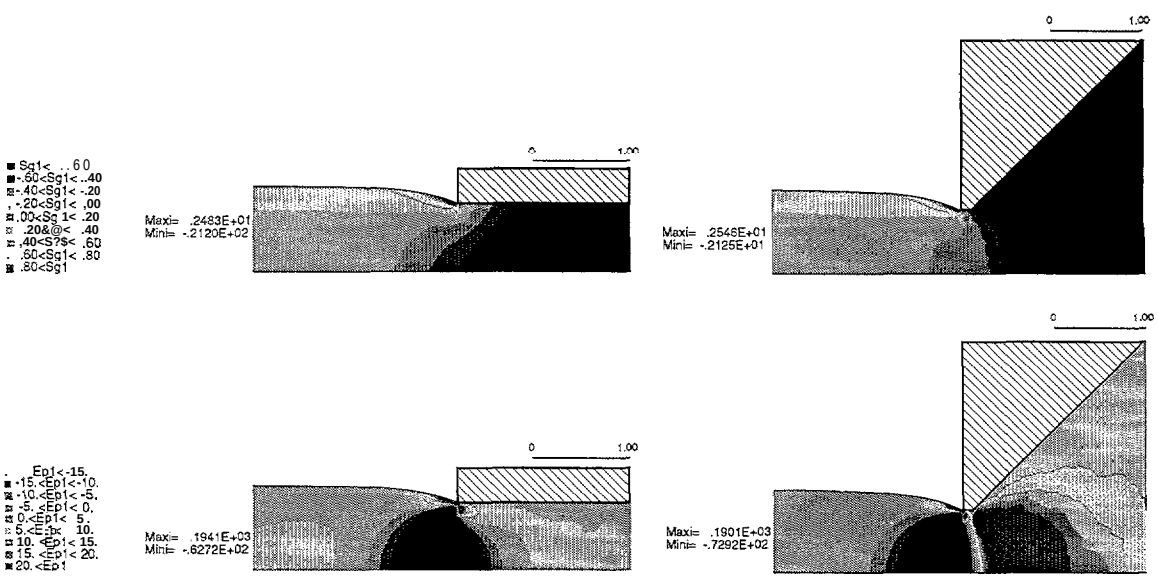

Fig. 8. Contour Enes of stretch rates (Ep1) and stress (Sg) along the streamlines, for resin CGC870, at a shear rate of 183 S-l.

originates at the die exit, it should be possible to understand which parameters control its onset and how it develops.

Typical contour lines of stretch rate and stress along the flow lines are shown in Fig. 8. The occurrence of high strain and stresses near the capillary exit is clearly visible. They may define areas where the flow is expected to break. Simulation have been performed for several resin rheology, at various flow rates. Qualitative predictions for the onset of surface defects have been obtained.

6. Process improvements and quantification

In order to validate the successive improvements for both the resin and the extrusion line, successive trials were performed. The starting point was the reference resin (A) and the initial extrusion line. The combination of progresses accomplished for the resin and the extrusion line has eventually allowed to reach the technological objectives for improved film blowing. A sketch of the extrusion blown film line is shown in Fig. 9.

From the machine point of view, next to the major improvements performed for the screw and the spiral mandrel die, a few additional minor improvements have also been done. A new winder with an increased take-up speed has been developed while the cooling system has been improved by using colder air. This improved cooling system is important, since it allows to keep a stable film bubble at high extrusion speed.

First of all, trials with the newly developed resin on the initial extrusion line have already led to some process improvements. However, the processing properties of this new resin are not fully exploited on this standard equipment which introduces some limiting factors.

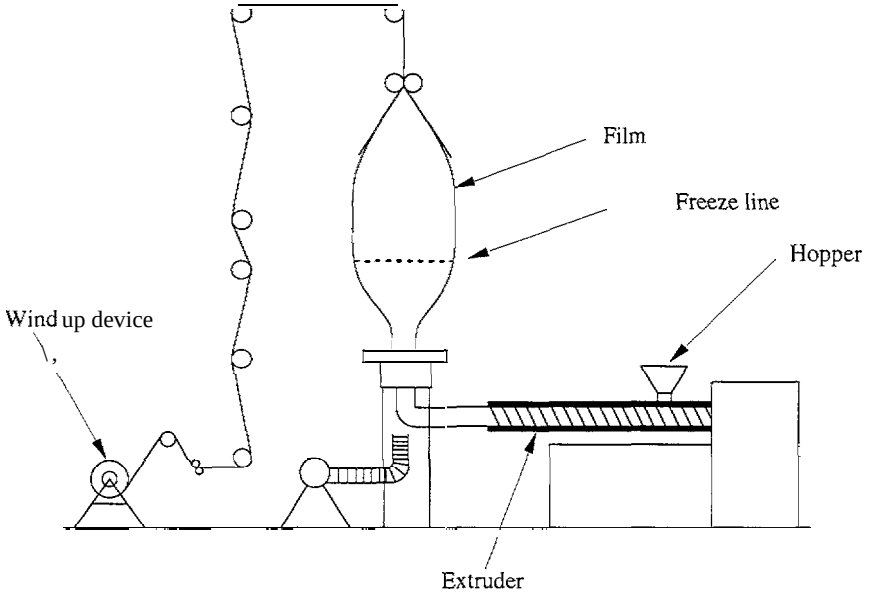

Fig. 9. Sketch of the film blowing process.

Fig. 10. Field application of mulch film. Automatic laying and tensioning (left) and photodegradation (right).

Still, excellent performances have been observed with resin C. This has suggested the production of an 8 μm thin film for field applications. Here, a photodegradable agent has been added to resin C. As compared to the 12 μm film produced with resin A, the new film did not show any difference in behaviour during the automatic laying and tensioning in the field. Fig. 10(a) shows a typical field application performed with resin C, while photodegradation can already be seen in Fig. 10(b).

Further trials performed on the new machine have shown significant progress. With the final resin D, very thin films were produced, the thickness of which is 6.9 μm, at a throughput of 300 kg/h. At a throughput of 360 kg/h, the minimum thickness was 7.9 μm : here the limiting factor is introduced by the maximum take-up speed of the winder. As long as cooled air is used, the bubble remains stable.

Thin films produced under several processing conditions have been analysed in order to identify their end-use properties. First of all, it is interesting to point out that the final LLDPE resin exhibits processing properties similar to an LDPE. In terms of end-use properties, at the maximum throughput of 360 kg/h, the end-use properties obtained with the final resin D show a slight decrease as compared with the reference resin A; however, they remain better than for the an LDPE.

7. Conclusions

A trans-national collaboration has been initiated between experts in complementary activities. It has been possible to tailor a new resin which exhibits enhanced processing properties in the context of film blowing. In depth analysis performed on the rheology, molecular structure and end-use properties have allowed to identify the best combination of molecular weight, distribution and branching.

Further, a blown film extrusion line has been optimised in order to achieve challenging objectives. Important parts have been reviewed and optimised. New design has been suggested for the screw, the spiral mandrel die ; tooling has followed. Also, other components of the extrusion line have

been improved in order to achieve the objectives: the bubble cooling system has been improved while a winder with a higher take-up speed is used.

The analysis and optimisation of the flow in a complex extrusion line is a challenge in itself. Complex 3-D geometries have required the development of a new solver with improved computational performances. Calculation speed-up have been obtained, making it feasible to simulate realistic and complex industrial flow situations.

Acknowledgement

The authors wish to acknowledge the European Commission for its financial support to this Brite-EuRam project accomplished under the contract number BRE2-CT92-0340.

References

1 K. Lowery, G.W. Knight, J.A. May, DOW patent GB-1500873-1,(1978)
2 R.S. Shipley, D.F. Birkelbach, DOW patent EP-53632-A,(1982)
3 B.S. Mientus, W.G. Fields, M.G. Bussey, DOW patent EP-109512-A,(I984)
4 L. P.P.M. Van der Heyden, DOW patent US-4542188-A, (1985)
5 V.S. Zabrocki, DOW patent EP-347794-A,(1989)
6 J.C. Stevens, D.R. Neithamer, DOW patent US-5064802-A,(1991)
7 W. Kaminsky, R. Spiehl, Makromol. Chem., 190 (1989) 515.
8 W. Kaminsky, H. Drögemüller, Makromol. Chem., Rapid Commun.,11(1990) 89.
9 W. Kaminsky, A. Bark, M. Arndt, Makromol. Chem., Macromol. Symp., 47 (1991) 83.
10 G.V. Vinogradov, A. Ya. Malkin, Yu. G. Yanovskii, E.K. Borisenkova, B.V. Yarlykov, G.V. Berezhnaya, J. Polym. Sci.,A-2,10 (1972) 1061.
11 B. Dickie, R.J. Koopmans, J. Polym. Sci., C,28 (1990) 193,
12. R.G. Larson, Constitutive equations for polymer melts and solutions, Butterworths (1988).
13. M.J. Crochet, B. Debbaut, R. Keunings and J.M. Marchal, in Applications of CAE in Extrusion and Other Continuous Processes, ed. K.T. O'Brien, Carl Hanser Verlag, München, 1992, chap. 2.
14. V. Legat and M.J. Crochet, Int. J. Num. Meth. in Fluids, 14 (1992) 609.
15. C.J.S. Petrie and M.M. Dem, AIChE, 22 (1976) 209.
16. G. Sornberger, J.C. Quantin, R. Fajolle, B. Vergnes and J.-F. Agassant, J. non-Newt. Fluid Mech., 23 (1987) 123.
17. P. Beaufils, B. Vergnes and J.-F. Agassant, Int. Polym. Proc., 5 (1990) 264.
18. J. Meissner and J. Hostettler, Rheol. Acts, 33 (1994) 1.
19. G. E. F'. Box, W.G. Hunter and J.S. Hunter, Statistics for experimentors, Wiley, New York (1978).
20. R. Koopmans, J. Polym. Sci, 26 (1988) 1157.
21. Trademark of TRANSVALOR, Sophia-Antipolis, France.
22. R.W. Freund, G.H. Golub and N.M. Nachtigal, Acts Numerica, (1992) 1.
23. A. Brand and J. Greenwald, Int. Series on Num. Math., 98 (1991) 143.
24. Y. Saad and M.H. Schulz, SIAM J. Sci. Stat. Comp., 7/3 (1986) 856.
25. D.M. Young and K.C. Jea, Linear Algebra and its applications, 34 (1980) 159.
26. 0. Axelsson, Linear Algebra and its applications, 29 (1980) 1.
27. A. Fortin, and M. Fortin, J. non-Newt. Fluid Mech., 36 (1990) 277.
28. B. Hendrickson and R. Leland, The chaco user's guide, version 1.0, Tech. Rep. SAND93-2339, Sandia National Laboratories, Albuquerque, NM, October 1993.
29. H. Schlichting, Grenzschicht-Theorie, Verlag G. Braun, Karlsruhe, 1968.
30. N. Phan Thien and R.I. Tanner, J. non-Newt. Fluid Mech., 2 (1977} 353.